Real World Modeling and Nonlinear Control of an Electrohydraulic Driven Clutch

M. A. Saeedi [1,*], R. Kazemi [2], M. Rafat [3], A. H. Pasdar [4]

[1] MSc Student, [2] Associate Professor, [3] MSc Student, [4] MSc Student, Department of Mechanical Engineering, K. N. Toosi University of Technology, Tehran, Iran.

[*] m_aminsaeidi@yahoo.com

Abstract

In this paper, a complete model of an electro hydraulic driven dry clutch along with its performance evaluation has elucidated. Through precision modeling, a complete nonlinear physical and full order sketch of clutch has drawn. Ultimate nonlinearities existent in the system prohibits it from being controlled by conventional linear control algorithms and to compensate the behavior of the system mainly during gearshift procedure, a nonlinear control program has been developed and tested. A unique approach to estimating clamp force has been adopted which makes the system comparable to a real world and full-physical one. Based on this type of modeling, the control approach is a true and feasible, ready-to-implement program which is based only on reality. The clutch model has been validated against experiments and great agreement has been attained since, every fine point has been taken into account and nothing is out of representation unless it is not crucial to system performance. The nonlinear control program does the control task very well and administrates the system in the desired trajectory.

Keywords: *Automated manual transmission, Electro hydraulic actuator, Nonlinear modeling, Nonlinear control, Precision modeling.*

1. INTRODUCTION

While Automatic Transmissions (AT) usually offer better shift quality and drivability, they do not perform in direction of optimum fuel economy. On the other hand, Manual Transmissions (MT) outperform ATs in the field of fuel economy but has worse gear shift quality [1]. But once MTs become automated, they can do both tasks very well. It is well known that using an electrohydraulic actuator along with proper control strategies can gratify both ends to a great extent. Electrohydraulic actuators are widely spread in many applications and are used in automated manual transmissions (AMT) too. While novel and powerful clutch systems like Dual Clutch transmissions (DCT) [2] have appeared, in the battle for lower weight and overall lower costs, single dry clutches has become more popular again. In the present paper, precision modeling of an electrohydraulic actuator besides mechanical parts of the single dry clutch has been explicated. Today, many researchers have studied the system from different points of view. A. Amir Ibrahim et al. [3] investigated use of a Multi-variable Linear Quadratic Optimal Control Theory for improving gear shift quality. Zhang et al. [4] studied the clutch system in a nonlinear model and adopted an adaptive-optimal control program to administer the system. G. Lucente et al. [5] considered modeling a servo-actuated clutch system. P. Dolcini et al. [6] made another research on optimal control of dry clutch engagement. Guihe Qin et al. [7] did a research on cruise control of AMT. J. Fredriksson, and B. Egardt [8] studied another nonlinear control algorithm for AMT. Hirohisa Tanaka and Hideyuki Wada [9] proposed a Fuzzy control algorithm for clutch engagement of AMT. K. Hayashi et al. [10] represented another Neuro fuzzy optimal transmission control for AMT. M. Montanari et al. [11] made a convincingly complete model of AMT and its electro hydraulic actuator and proposed a controller for its compensation. L. Glielmo et al. [12] proposed another modeling of servo-actuated clutch system as well as a control program. Gianluca Lucente et al. [13] represented an outstanding AMT model along with a gearbox and

driveshafts model. There are other researches that carried out on a vehicle with hybrid configuration. In these researches, the electrical motor has been used as a beneficial component in improving shift quality and facilitating the control task. Sung-tae Cho et al. [14] researched into AMT shift control in a hybrid drivetrain. Ye Ming et al. [15] studied on startup strategies in a hybrid electrical vehicle equipped with AMT. R. C. Baraszu and S. R. Cikanek [16] made another research regarding use of electrical motor as a fill-in torque producer during AMT gear shift. While these researches have focused on general clutch control of AMT, there are other researches that have made use of more pristine concepts like Integrated Powertrain Control (IPC) and use of engine for gearshift actuation. M. Pettersson and L. Nielsen [17] introduced a gear shift strategy based on engine control rather than clutch control. Jonas Fredriksson and Bo Egardt [18] made another research regarding use of nonlinear IPC for gear shifting of an AMT. Although there have been fairly plenty researches regarding AMT modeling and its control techniques, most of studies betray lack of necessary fine points. During engagement of clutch, the most important factor which drastically affects system performance is compensation of clamp force. Keeping in mind that the engagement process only acts in less than 1mm travel of pressure plate, it makes any modeling that has not considered this real world key factor, futile. For such a highly nonlinear model, sophisticated control programs are feasible only when the modeling is based on reality.

In the present paper, a complete real world model of the AMT and its associated electrohydraulic actuator in a general case has drawn. The model has been validated against experiments and then a truly applicable nonlinear control program for gearshift procedure based on analytical findings rather than experiments which might not suit all situations, has been developed.

2. CLUTCH MODELING

Since the engine and driveline components are getting downsized more and more, single dry clutch has become of interest again. However, this type of clutch is highly nonlinear and if any control approach intends, the modeling must be physical and full-order otherwise the control program will not be feasible. A schematic representation of the clutch system is shown in Fig. 1. The clutch is composed of servovalve, pipeline and hydraulic-mechanical actuator.
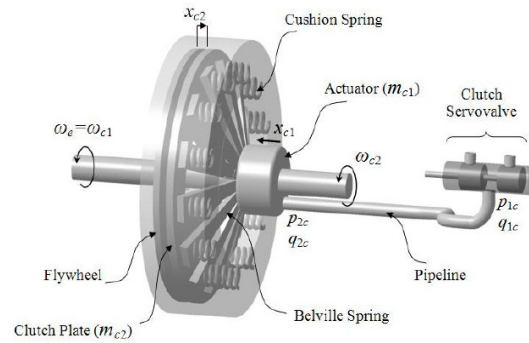

Fig1. Schematic drawing of the clutch system including servovale, pipeline and electrohydraulic actuator.

3. Servovalve Model

Electrohydraulic actuators are widely spread in many applications. In view of the fact that lower overall cost is an objective in the automobile industry, this sort of actuator is mainly used in semi-automatic transmissions. Following valuable modeling represented in [11], the servovalve considered here is a three-way spool flow control valve [20]. It consists of a plunger moved by an electromagnetic actuator. The plunger displacement defines the supply and return orifice areas. It is moved by spring forces (which maintain the load connected to the return when no external force is applied) and forces generated by the electric actuator. Servovalve model refers to three subsystems: mechanical, electromagnetic and hydraulic.

4. Mechanical model

Dynamics of mechanical model of the servovalve can be described as[4]:

$$m_{vc}\ddot{x}_{vc} = -F_{0c} - k_c x_{vc} - b_{vc}(v_{vc}) + f_{mc}(x_{cv}, \varphi) + F_{Bc}(x_{vc}, p_{1c}, p_s, p_0) \qquad (1)$$

where m_{vc} represents the plunger mass, x_{vc} and v_{vc} are the plunger position and velocity respectively, $F_{0c} + k_{vc}x_{vc}$ denotes for valve spring forces, $b_{vc}(v_{vc})$ represents the total friction forces (viscous + static +Coulomb) acting on the plunger owing to oil flowing in the valve restrictions, F_{Bc} is the Bernoulli force applied on the plunger due to fluid flowing through orifices and f_{mc} represents the electromagnetic force. The Bernoulli force is described as follows[4]:

$$F_{Bc} = \begin{cases} C_{dv}A_{fc}(x_{vc})|p_s - p_{1c}|, & x_{vc} > x_{vc-filling} \\ 0, & x_{vc-dumping} \leq x_{vc} \leq x_{vc-filling} \\ -C_{dv}A_{dc}(x_{vc})|p_{1c} - p_0| & x_{vc} < x_{vc-dumping} \end{cases} \qquad (2)$$

where C_{dv} is a constant showing geometry structure parameter, A_{fc} and A_{dc} are the filling and dumping orifice areas and $x_{vc-filling}$ and $x_{vc-dampin}$ define amplitude of the dead zone. p_s and p_0 represent pressures of high pressure reservoir and low pressure tank correspondingly to which the servovalve is connected and p_{1c} denotes upstream pressure. Bernoulli forces are proportional to the orifice area and the pressure drop and always act in a direction to close the orifice.

Electromagnetic model: The electromagnetic force which is applied to the plunger is created by a variable reluctance actuator, constituted by a solenoid and a slider connected to the plunger. Detailed structure of the electromagnetic model is defined in [21].

$$\dot{\varphi} = \frac{1}{N}(V - ri_c) \tag{3}$$

$$Ni_c = \begin{bmatrix} R(x_{vc})\varphi \\ +X(\varphi) \end{bmatrix} \tag{4}$$

$$f_{mc}(x_{vc},\varphi) = -\frac{1}{2}\frac{\partial R}{\partial x_{vc}}(x_{vc})\varphi^2 \tag{5}$$

where N is the number of coil turns, $N\varphi$ is the linked magnetic flux, i_c is the winding current, V is the input voltage, r is the winding resistance, $R(x_{vc})$ is the nonlinear air-gap reluctance and $X(\varphi)$ is the nonlinear magnetization curve of the iron core.

However, for the sake of lowering needed numerical calculation, the magnetic force $f_{mc}(x_{vc},\varphi)$ can be found by solving a linear first order differential equation which directly relates the force to the valve current:

$$\dot{f}_{mc} = -\frac{f_{mc}}{\tau_c} + \frac{k_c \cdot i_c}{\tau_c} \tag{6}$$

where τ_c denotes electro-magnetic time constant and k_c refers to an electro-mechanical constant.

5. Hydraulic Model

The valve is an overlapped valve i.e. the land width is greater than the port width in neutral mode, when there is no oil flow. Thus, there is a dead band in the orifice area vs. spool displacement as depicted in Fig. 2. The servovalve outlet flow can be written according to Bernoulli's equation q_{1c} where C_d is the discharge coefficient and ρ is the oil density.

$$q_{ic} =$$
$$\begin{cases} C_d\sqrt{\frac{2}{\rho}}\text{sign}(p_s - p_{1c})\sqrt{|p_s - p_{1c}|}A_{fc}(x_{vc}), & x_{vc} > x_{vc-filling} : \text{filling} \\ 0, & x_{vc-dumping} \leq x_{vc} \leq x_{vc-filling} : \text{dead zone} \\ -C_d\sqrt{\frac{2}{\rho}}\text{sign}(p_{1c} - p_0)\sqrt{|p_{1c} - p_0|}A_{dc}(x_{vc}), & x_{vc} < x_{vc-dumping} : \text{dumping} \end{cases} \tag{7}$$

6. Pipeline Model

Due to car lay-out constraints, pipeline can be relatively long and flexible. Delay owing to propagation of the flow in the line and pressure/flow oscillations must be taken into account when the pipeline is excited with the large bandwidth inputs required for the clutch movement. Moreover, pipeline and actuator chamber introduce complex and quite uncertain dynamics in the system, since oil parameters are temperature dependent and some hydraulics effects cannot be well modeled. In order to guarantee robust stability of any closed-loop control system, a careful analysis of the pipeline dynamics is necessary. These dynamics strongly affect the achievable system performance.

Using a scattering variables approach, it is possible to model the fluid line as a two-port network with inputs and outputs given by the upstream and downstream flows q_{1c} and q_{2c} and pressures p_{1c} and p_{2c} . Since the natural output of the valve is the oil flow q_{1c}, while the input of the actuator is the oil flow q_{2c}, the two-port configuration shown in Fig. 3 is used. Having solved PDEs describing the fluid line [22,23], and model approximation techniques [24,25], the following reduced-order finite-dimensional LTI model for the fluid line is obtained:

$$\begin{bmatrix} P_{1c}(s) \\ Q_{2c}(s) \end{bmatrix} = \sum_{i=1}^{j} \begin{bmatrix} \frac{(-1)^{i+1}(2/D_j)\lambda_{ci}}{\bar{s}^2 + 8\bar{s} + \lambda_{ci}^2} & \frac{(2Z_0/D_j)(\bar{s}+8)}{\bar{s}^2 + 8\bar{s} + \lambda_{ci}^2} \\ \frac{(2Z_0/D_j)\bar{s}}{\bar{s}^2 + 8\bar{s} + \lambda_{ci}^2} & \frac{(-1)^{i+1}(2/D_j)\lambda_{ci}}{\bar{s}^2 + 8\bar{s} + \lambda_{ci}^2} \end{bmatrix} \times$$
$$\begin{bmatrix} P_{2c}(s) \\ Q_{1c}(s) \end{bmatrix} \tag{8}$$

where

$$D_j = \frac{lv_0}{c_0r_0^2}, \quad Z_0 = \frac{\rho_0c_0}{\pi r_0^2}, \quad \bar{s} = \frac{r_0^2}{v_0}s, \quad c_0 = \sqrt{\frac{\beta_e}{\rho_0}}$$

$$\lambda_{ci} = \left(i - \frac{1}{2}\right)\frac{\pi}{D_j}, \quad i = 1,2,\dots,j$$

and j is the number of modal frequencies λ_{ci}, l is the axial length of the pipeline, r_0 represents the radius of the tube, ρ_0 is the oil density, β_e denotes the equivalent oil bulk modulus in the pipeline taking into account pipeline elasticity, c_0 is the sonic velocity of the fluid and v_0 is the mean kinematic viscosity. It should be noted that the hydraulic circuit is provided with a spilling device that ensures there is no significant amount of air enclosed in the pipe. Hence, the effect of entrained

air can be neglected. Simulations show that $j = 6$ modes are adequate to converge the solution.
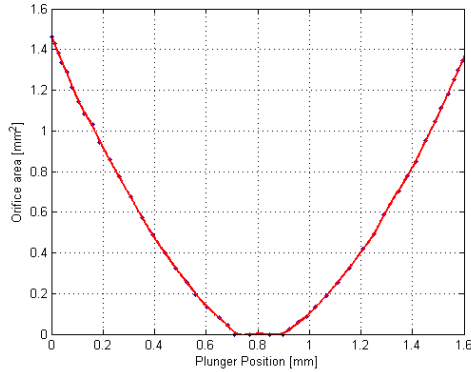

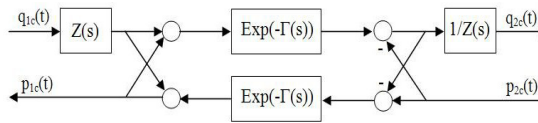**Fig2.** Graph of clutch servovalve orifice area vs. plunger position.

Fig3. Schematic of the two-port network used for pipeline model.

7. Hydraulic-Mechanical Actuator Model

The automated clutch consists of a standard single dry clutch controlled by an elctrohydraulic servo system described before. As shown in Fig. 1it is comprised of the actuator driven release bearing which pushes on Belville springs. Sun-like Belville springs act both as spring and variable coupling ratio levers [26]. When no external force is applied, by means of cushion springs, flywheel and clutch plate are firmly pressed together and a definite amount of torque is flowing through the clutch. Once pressure applied to the release bearing by the hydraulic actuator, the movement of the release bearing is transmitted through the Belville springs to the clutch plate and makes it detached from flywheel so that torque flow can be lowered or be disconnected and gear engagement or disengagement occur. By adjusting the gap between clutch plate and flywheel, the transmitted torque from the engine to the gearbox can be compensated.

The ultimate nonlinearities and hysteresis in Bellvile and cushion springs as well as existence of damping and friction besides this fact that the engagement process only act in the last 0.7 mm travel of the pressure plate [26], makes it hardly possible to control the transmitted torque. However, these phenomena must be considered if a complete model for capturing the best performance

is needed. Study of the literature shows that these characteristics have not been considered together in a full model so far.
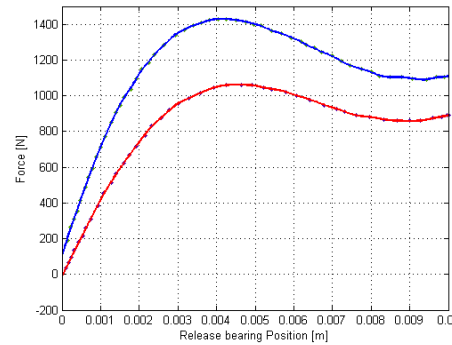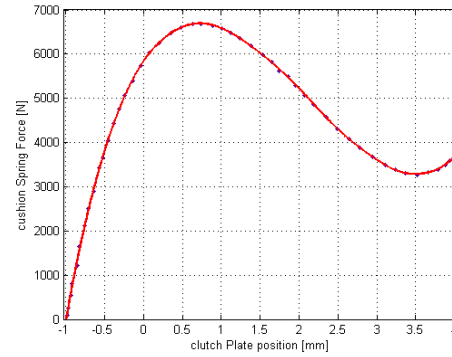

Fig4. Cushion spring characteristic and hysteresis phenomenon in Belville springs

The governing equations are as follow [11]:

$$\dot{p}_{2c} = \frac{\beta}{V_{0c} + A_c x_{c1}}(q_{2c} - A_c v_{c1}) \qquad (9)$$

$$m_{c1}\ddot{x}_{c1} = -b_{c1}v_{c1} - f_b(x_{c1}, v_{c1}) + A_c p_{2c} \qquad (10)$$

$$m_{c2}\ddot{x}_{c2} = -b_{c2}v_{c2} + c_r f_b(x_{c1}, v_{c1}) - f_{cu}(x_{c2}) + n_c(x_{c2}) \qquad (11)$$

$$f_b(x_{c1}, v_{c1}) =$$
$$\begin{cases} f_{be}(x_{c1}), & (v_{c1} > 0) \text{ or } (v_{c1} = 0, \text{ and } -b_{c1}v_{c1} + A_c p_{2c} > f_{be}(x_{c1})) \\ -b_{c1}v_{c1} + A_c p_{2c}, & f_{be}(x_{c1}) \leq -b_{c1}v_{c1} + A_c p_{2c} \leq f_{be}(x_{c1}) \quad (12) \\ f_{bc}(x_{c1}), & (v_{c1} < 0) \text{ or } (v_{c1} = 0, \text{ and } -b_{c1}v_{c1} + A_c p_{2c} < f_{bc}(x_{c1})) \end{cases}$$

where β is the bulk modulus of the oil, V_{oc} is the minimum volume of the chamber, A_c denotes actuator cross sectional area, x_{c1} , v_{c1} and x_{c2} , v_{c2} refer to release bearing (which is connected to the clutch actuator) and clutch plate positions and velocities, m_{c1}, m_{c2} represent the actuator and the clutch plate masses, b_{c1} and b_{c2} correspond to damping coefficients for the release bearing and the clutch plate, $f_b(x_{c1}, v_{c1})$ and $f_{cu}(x_{c2})$ are nonlinear forces that emerge from Belville and cushion springs. c_r is the coupling ratio of the Belville spring and finally n_c represents the normal force acting on the pressure plate. The function $f_{cu}(x_{c2})$ has totally recorded according to

experimental evaluation and there is an analytical expression for $f_b(x_{c1}, v_{c1})$ shown in equation (12) where $f_{be}(x_{c1})$ and $f_{bc}(x_{c1})$ as well as $f_{cu}(x_{c2})$ are experimental functions represented in Fig. 4.

8. Clamp Force Estimation

The most important part of clutch modeling which is extremely crucial to system performance and has been neglected by most of studies is clamp force estimation. To bring off in modeling of last-travel-engagement of the clutch plate discussed, the clamping load n_c has been adopted by a linear function of x_{c2} with a negative slope and is limited between its maximum value just when the clutch is fully engaged and zero

$$n_c(x_{c2}) = \begin{cases} -k_1 x_{c2} + k_2, & 0 \leq x_{c2} < 7e-4 \\ 0, & x_{c2} \geq 7e-4 \end{cases} \quad (13)$$

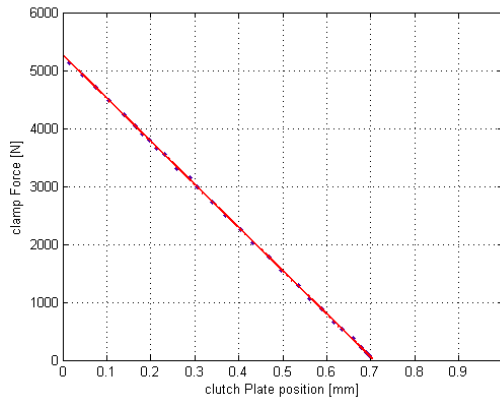where k_1 and k_2 are positive constants.

Fig5. Variation of clamp load in terms of clutch plate position

This adoption makes a fairly complete description of clamp force (see Fig. 5), however, if a more accurate explanation intends, experiments should take place. Through experiments, one can obtain an exact relation for $n_c(x_{c2})$ which is going to correctly sketch full characteristics of the clamp load during the engagement process. In the present study, the linear function is used throughout the paper.

9. Friction Torque Capacity

One of the important parts of the modeling is friction torque description of the clutch. Several complete models have been proposed in the literature [27-31] and in the present paper, based on the well-known stick-slip representation of the friction effect [27], the following real-world model is employed:

$$T_c = \begin{cases} -min(T_e, R \times \mu \times n_c), & \omega_{rel} < -\omega_0 \\ s \times \omega_{rel}, & -\omega_0 < \omega_{rel} < \omega_0 \\ min(T_e, R \times \mu \times n_c), & \omega_{rel} > \omega_0 \end{cases} \quad (14)$$

where T_c is the friction torque, T_e shows the engine torque input into the clutch, ω_{rel} denotes relative angular velocity between flywheel and the clutch plate, ω_0 is the threshold of the relative angular velocity which divides and defines stiction-slip regions and R is the mean friction contact radius.

$$s_c = \frac{T_c|_{\omega_{rel}=\omega_0}}{\omega_0} \quad (15)$$

Defining linear variation of the transmitted torque T_c when $|\omega_{rel}| < \omega_0$, corresponds to the stiction region while the other case represents the slip region. In the slip region, μ is the variable coefficient of friction which is derived from friction characteristics of the lining material and can be described as a function of relative linear velocity at the mean friction radius:

$$\mu = c_4 \times v_{rel}^3 + c_3 \times v_{rel}^2 + c_2 \times v_{rel} + c_1 \quad (16)$$

where $v_{rel} = R \times \omega_{rel}$ and c_1, c_2, c_3 and c_4 are the coefficients of the third-order polynomial adapted to the friction material model. It should be noted that the friction torque T_c cannot be higher than the input engine torque T_e, when the engine acts as an actuator.

It should also be mentioned that this model is not adequate for proper investigation of judder phenomenon and a higher level of modeled dynamics will be required [26].

10. Model Validation

Following the same procedure for parameter identification presented in [11], the real clutch parameters have been identified and empirical data have been extracted. Then, under equal operating conditions, comparisons between experiments and simulation have been performed. To aim at this, a sample current i_c has been given both to the real platform and simulation system and thereby clutch movements have recorded. Fig. 6 shows the sample current as well as x_{c1} and x_{c2} and clamp load n_c for both experiment and simulation. The simulation results demonstrate excellent agreement with empirical data, expressing great level of dynamics modeled.
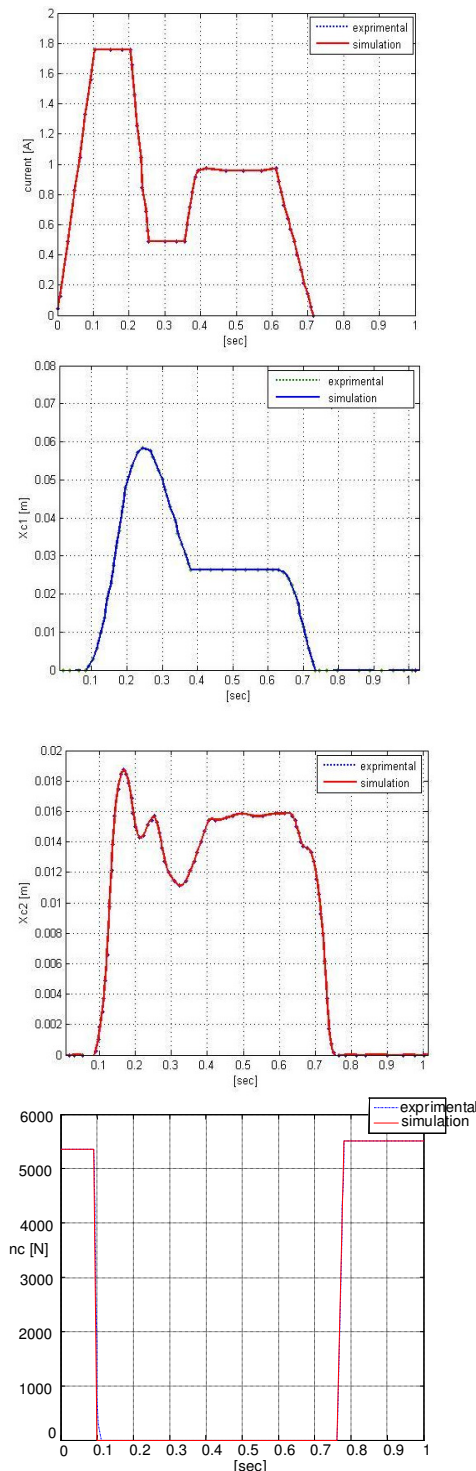
Fig6. Sample input current and simulation (-) and experimental (.) results for the clutch system

11. CONTROLPROGRAM DERIVATION

In order to compensate the proposed model, a nonlinear control program to control the gearshift process has been adopted.

The control programs proposed in the literature aimed at a modest and even low-detailed model and cannot be applied for the detailed presented model.

During the last phase of gear shift procedure, just after the gear changed and gearbox synchronized, the clutch is going to lock so that the torque can flow from the engine to the wheels. After changing gear, there are two different speeds on the flywheel and the clutch plate and this speed difference have to be ironed out, i.e. the clutch synchronizes. As mentioned, there have been researches based on gear shifting just by engine control or Integrated Power Control scheme [14-18]. These approaches are feasible mainly in hybrid drive-trains in which the difference can helpfully be lowered by adjusting the speed difference "externally" i.e. by engine or electric motor actuation. However, in general case of control of an AMT, what the present study aims at, this difference has to be mostly disappeared by making frictional contact which clutch plate produces while it touches flywheel. In other words, clutch synchronization would synchronize the speeds by itself. This makes the control program much more complicated as an appalling shuffle would emerge by an unsuccessful engagement.

The control strategy is based on "smooth clutch engagement" i.e. this fact that the clutch plate should make contact with flywheel as smooth as possible. Yet again, it should be mentioned that the engagement process should be done in the least time span possible as the drive ability is going to decrease when the engagement time increases. These facts stipulate that the clamp force n_c should increase in a smooth way from its minimum when the clutch plate is detached, to its maximum when the clutch is fully engaged. Since this action is going to happen only in 0.7 mm, the control program must draw a careful and detailed attention.

12. Control Model

In order to develop an efficient yet precise and feasible control program, first, a simplified form of some parts of the clutch model has been extracted and the other crucial parts of model have directly been inserted into the control model. The servovalve model has been simplified and the steady state response of its mechanical model is used in which the Bernoulli force has been neglected and the electromagnetic force acting on

the servovalve plunger is considered proportional to the valve current through a force constant K_{fc}:

$$x_{vc} = (-F_{0c} + K_{fc}i_c)/k_c \qquad (17)$$

The pipeline model is inserted in its intact form. Since the control program intends to compensate the clamp force only in 0.7 mm travel, the uncertain dynamics in the pipeline must draw attention. Use of any simplified form of the pipeline would cause in intolerable errors and the program would fail especially when small displacements of the clutch plate intend. The hydraulic-mechanical actuator model is involved in the control program almost in its original form except for a simplified relation of the $f_b(x_{c1}, v_{c1})$:

$$f_b(x_{c1}, v_{c1}) = f_b(x_{c1}) = \frac{1}{2}(f_{be}(x_{c1}) + f_{bc}(x_{c1})) \qquad (18)$$

As it will be discussed later, this simplification is mostly done because of facilitating extraction of x_{c1d} or the desired trajectory of the release bearing.

13. Control Algorithm

Based on Backstepping methodology [32,33] and through virtual control signals, the clamp force n_c is controlled by means of electrohydraulic current i_c as it is done in reality. Since the control program compensates the clamp force n_c, first, a desired n_c is set. Based upon the desired clamp load n_{cd} which implies "smooth engagement", the desired clutch plate trajectory x_{c2d} according to (13) is set:

$$x_{c2d} = \frac{k_2 - n_{cd}}{k_1}, \qquad 0 < n_{cd} < n_{cd-max} \qquad (19)$$

Hereafter, through taking intermediate variables as virtual control signals, the midway desired signals appear and finally the real control signal will be obtained.

The desired x_{c1} can be acquired by backstepping the x_{c2d}. Hence, derived from (11), the desired trajectory of x_{c1} i.e. x_{c1d} is obtained according to the following equation[26]:

$$f_b(x_{c1d}) = (m_{c2}\dot{v}_{c2d} + b_{c2}v_{c2d} + f_{cu}(x_{c2d}) - n_c(x_{c2d}))/c_r \qquad (20)$$

Solving the above equation, one can obtain x_{c1d} as the desired release bearing trajectory. However, as depicted in Fig.4, the functions $f_{bc}(x_{c1})$ and $f_{be}(x_{c1})$ are not invertible. To overcome this problem, the decision on inversion is done by considering other clutch variables too. Having been determined desired release bearing position, the following equations govern the way up to the desired current control signal. Supposing

position and velocity errors of the release bearing as $\tilde{x}_{c1} = x_{c1} - x_{c1d}$ and $\tilde{v}_{c1} = v_{c1} - v_{c1d}$:

$$v_{c1d} = \dot{x}_{c1d} - k_x\tilde{x}_{c1} \qquad (21)$$

where k_x is a strictly positive constant showing position regulator. Defining so, the position error of release bearing becomes

$$\dot{\tilde{x}}_{c1} = -k_x\tilde{x}_{c1} + \tilde{v}_{c1} \qquad (22)$$

Considering relation (10),the following defines derivative of the velocity error:

$$\dot{\tilde{v}}_{c1} = \frac{1}{m_{c1}}(-b_{c1}v_{c1} - f_b(x_{c1}) + A_c p_{2c}) - \dot{v}_{c1d} \qquad (23)$$

And one might extract the desired downstream pressure as follows:

$$p_{2cd} = \frac{b_{c1}}{A_c}v_{c1} + \frac{f_b(x_{c1})}{A_c} + \dot{v}_{c1d}\frac{m_{c1}}{A_c} - k_v(x_{c1} - x_{c1d}) \qquad (24)$$

where k_v is another strictly positive constant showing velocity regulator. Supposing $\tilde{p}_{2c} = p_{2c} - p_{2cd}$ as the downstream pressure error, the following determines the release bearing velocity error:

$$\dot{\tilde{v}}_{c1} = -\frac{A_c}{m_{c1}}k_v\tilde{v}_{c1} + \frac{A_c}{m_{c1}}\tilde{p}_{2c} \qquad (25)$$

Considering equation (9):

$$\dot{\tilde{p}}_{2c} = \frac{\beta}{V_{0c} + A_c x_{c1}}(q_{2c} - A_c v_{c1}) - \dot{p}_{2cd} \qquad (26)$$

So the following relation defines the desired downstream flow:

$$q_{2cd} = A_c v_{c1} + \dot{p}_{2cd} \times \frac{V_{0c} + A_c x_{c1}}{\beta} - k_p\tilde{p}_{2c} \qquad (27)$$

where k_p is another strictly positive constant denoting pressure regulator. The error function of downstream pressure becomes:

$$\dot{\tilde{p}}_{2c} = -\frac{k_p\beta}{V_{0c} + A_c x_{c1}}\tilde{p}_{2c} + \frac{\beta}{V_{0c} + A_c x_{c1}}\tilde{q}_{2c} \qquad (28)$$

where downstream flow error is defined as $\tilde{q}_{2c} = q_{2c} - q_{2cd}$.
Using the full pipeline model (8), one might resolve the governing equations with q_{2cd} and p_{2c} as input and obtain p_{1cd} and q_{1cd} . Having obtained desired upstream pressure and flow, the relation (29) derived from inversion of equation (7) produces the desired servovalve plunger position.

$$x_{vcd} = \begin{cases} A_{fc}^{-1}\left(\dfrac{q_{1cd}}{c_d\sqrt{2/\rho}\sqrt{|p_s - p_{1c}|}}\right), & q_{1cd} > 0 \\ (x_{vc-filling} + x_{vc-dumping})/2, & q_{1cd} = 0 \\ A_{fc}^{-1}\left(\dfrac{q_{1cd}}{c_d\sqrt{2/\rho}\sqrt{|p_{1c} - p_0|}}\right), & q_{1cd} < 0 \end{cases} \qquad (29)$$

Finally, the desired current control signal i_{cd} can be achieved using the simplified model of servovalve defined in (17).

Performance Evaluation

In this section, the developed control program is implemented and its performance is analyzed. No real experiments have been performed and only via simulation the behavior of the clutch system in presence of the controller is evaluated.

Fig. 7 shows the behavior of the clutch system under control along with its desired trajectories set. In order to get a good tracking, k_x, k_v and k_p have been replaced with many possibilities and through trial and error a good set have opted. The results show that the control program has done well within an acceptable time and is able to compensate such a highly nonlinear model. Regarding stability of the proposed controller, the equation system of errors (22), (25) and (28) has negative eigenvalues and stabilizes the origin. The proof of stability can be done through taking a simple Lyapunov function and manipulating its differentiation in order to reach an always (conditional) negative response. Since governing equations of the controller are lengthy, this process is not stated here for the sake of space.

As it is clear in the results, the system does not strictly follow the desired trajectories. In fact, this behavior can be modulated by modifying the gain set. However, remembering "smooth engagement" control strategy, the behavior of the system should comply with being "smooth" rather than strictly following the desired routes.

It should be noted that the nature of the control algorithm used implies that higher oscillatory response would emerge if a fully strictly following reaction intends.

Although the results of tracking performance evaluation have proved satisfactory, one more simulation is needed to determine whether the control program can prevent driveline from producing unwanted torsional vibrations. To aim at this, a simplified driveline model has been assumed and the last phase of the gear shift procedure i.e. clutch synchronization, has been simulated again.

It is supposed that the new gear has engaged so there are two different rotational speeds on flywheel (engine speed) and clutch plate (gearbox and vehicle speed).
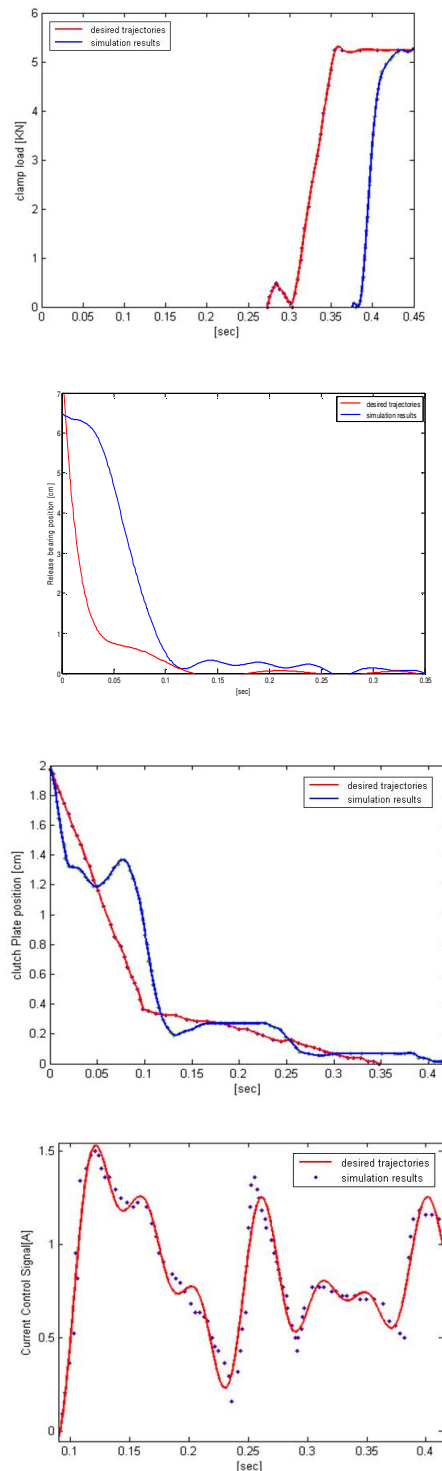

Fig7. Tracking performance evaluation of the controller. The red lines correspond to the desired trajectories while the blue ones show the simulation results.

The following describes mathematical description of the simple driveshafts model used for testing, when the gearbox has just synchronized and the clutch is ready to engage:

$$J_{c1}\dot{\omega}_{c1} = T_e - T_c \,,$$

$$J_{c2}\dot{\omega}_{c2} = T_c - T_{cg} \,,$$

$$J_{ge}\dot{\omega}_g = T_{cg} - b_g\omega_g - \frac{T_{gw}}{r_g} \,, \tag{30}$$
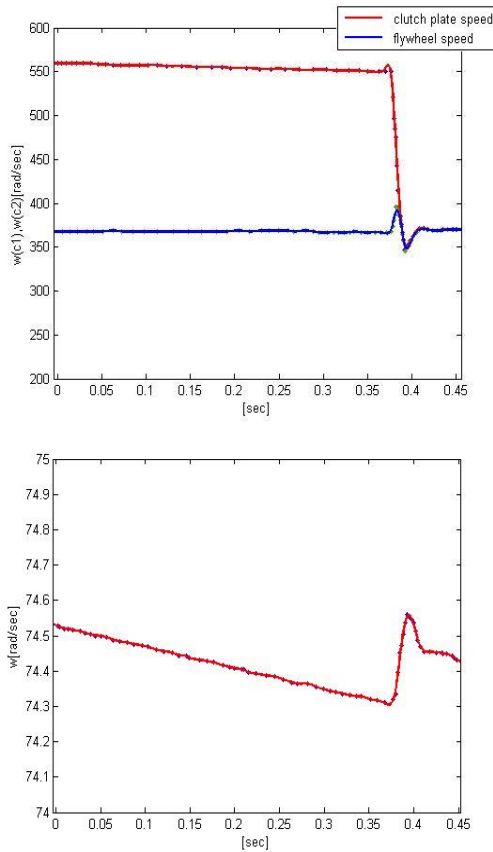

Fig8. The shuffle test results. On the left figure, the red line corresponds to the flywheel (engine) speed and the blue line denotes clutch plate speed. The right figure shows wheel speed.

$$J_w\dot{\omega}_w = T_{gw} - T_r \,,$$

where T_e is the torque produced from engine and T_c corresponds to the clutch torque:

$$T_{cg} = k_{cg}\theta_{cg} + b_{cg}\omega_{cg} \,, \theta_{cg} = \omega_{cg} = \omega_{c2} - \omega_g$$

$$T_{gw} = k_{gw}\theta_{gw} + b_{gw}\omega_{gw} \,, \dot{\theta}_{gw} = \omega_{gw} = \omega_g - \omega_w \tag{31}$$

where ω_{c1} , ω_{c2} denote flywheel (engine) angular speed and clutch plate angular speed, T_{cg} and T_{gw} represent viscoelastic torques transmitted

through main shaft and secondary shaft respectively. b_g is damping existent in the main shaft support. r_g is the gear ratio and k_{cg} , k_{gw} and b_{cg} , b_{gw} are equivalent shaft stiffness and damping in main and secondary shafts correspondingly. ω_g, ω_w show input speed of the engaged gearbox and wheel rotational speed respectively. J_{c1} , J_{c2} , J_{ge} , J_w represent equivalent inertias of the flywheel, clutch plate, gearbox and wheel correspondingly and T_r denotes opposing torques to the wheel. At this time, the Initial condition defining two different speeds on the clutch sides is set and the tracking control program presented is fed into the system.

Fig. 8 demonstrates the history of clutch and wheel speeds during clutch engagement. The outputs represent promising results and once again the control program revealed its true suitability for compensating such a sophisticated system. Change of speeds due to shuffle is low enough (8% of the initial speed) to be neglected and a smooth engagement has been made.

14. CONCLUSION

A detailed, real-world model of a dry clutch system along with its actuator modeling has been expounded. True description of the model is a key factor to future control plans so the present study aimed at precision modeling. Based only on real, existent phenomena, every necessary fine point was counted in. Unlike the literature, the most important part of a clutch model i.e. clamp load drew a careful attention. Modeling reality, a real and truly feasible control plan was implemented. Though the model is complicated, the nonlinear control program proved good and satisfactory results. While detailed modeling is a burden, its beneficial effects can be very inspiring. The control program developed in this paper is truthfully doable and can remove the need for extra experiments and investigations in the next phases of production and manufacturing.

REFERENCES

[1]. Gunther Alvermann "Virtuelle Getriebeabstimmung", Shaker Verlag, Schriftenreihe des Instituts für Fahrzeugtechnik, TU Braunschweig, Dissertation, 2009.

[2]. Y. Zhang, X. Chen, X. Zhang, H. Jiang, W. Tobler, "Dynamic Modeling and Simulation of a Dual-Clutch Automated Lay-Shaft Transmission," Journal of Mechanical Design, 127,2, pp. 302-307, 2005.

[3]. A Amir Ibrahim, Qin Datong, Liu Zhenjun, Ye Ming, "An Improvement in the Shift Quality for Automatic Manual Transmissions Using Multi-variable Linear Quadratic Optimal Control Theory," Information Technology Journal. Vol. 4, no. 3, pp. 239-245. July 2005.

[4]. Zhang, L Chen, G Xi, "System dynamic modeling and adaptive optimal control for automatic clutch engagement of vehicles," Proceedings of the Institution of Mechanical Engineers, Part D: Journal of Automobile Engineering, 216, 983-991, 2002.

[5]. G. Lucente, M. Montanari, C. Rossi, "Modeling of a Car Driveline for Servo-Actuated Gear-Shift Control, "Industrial Electronics, 2005. ISIE 2005. Proceedings of the IEEE International Symposium on,1, 279-286, 2005.

[6]. P. Dolcini, H. Bechart, C. Canudas de Wit, "Observer-based optimal control of dry clutch engagement," Decision and Control, 2005 and 2005 European Control Conference. CDC-ECC '05. 44th IEEE Conference on, 440-445, 2005.

[7]. Guihe Qin, Anlin Ge, Jiehong Zhao, Ju-Jang Lee, "Cruise control of automated manual transmission vehicles," Computing & Control Engineering Journal, 14(2), 18-21, 2003.

[8]. J. Fredriksson, B. Egardt, "Nonlinear control applied to gearshifting in automated manual transmissions," Decision and Control, 2000. Proceedings of the 39th IEEE Conference on Publication Date: 2000, 1, 444-449, 2000.

[9]. Hirohisa Tanaka, Hideyuki Wada, "Fuzzy control of clutch engagement for automated manual transmission," Vehicle System Dynamics, Vol. 24, no. 4-5, pp. 365-376. 1995.

[10]. K Hayashi, Y Shimizu, S Nakamura, Y Dote, A Takayama, A Hirako, "Neuro fuzzy optimal transmission control for automobile with variable loads," IECON PROC, IEEE, COMPUTER SOCIETY PRESS, LOS ALAMITOS, CA (USA), 1,430-434, 1993.

[11]. M. Montanari, F. Ronchi, C. Rossi, A. Tilli, A. Tonielli, "Control and performance evaluation of a clutch servo system with hydraulic actuation," Control Engineering Practice, 12, 1369–1379, 2004.

[12]. L. Glielmo, L. Iannelli, V. Vacca,F.Vasca, "Gearshift control for automated manual transmissions," Mechatronics, IEEE/ASME Transactions on, 11 (1), 17-26, 2006.

[13]. Gianluca Lucente, Marcello Montanari, Carlo Rossi, "Modeling of an automated manual transmission system," Mechatronics, 17, 73–91, 2007.

[14]. Sung-tae Cho, Soonil Jeon, Han-San Jo, Jang-Moo Lee, Yeong-Il Park, "A development of shift control algorithm for improving the shift characteristics of the automated manual transmission in the hybrid drivetrain," International Journal of Vehicle Design,26 (5), 469-495, 2001.

[15]. Ye Ming, Qin Datong, Liu Zhenjun, "Research on starting up strategies of mild hybrid electric vehicle equipped with automatic manual transmission," Zhongguo Jixie Gongcheng, 16 (5), 442-445, 2005.

[16]. Di Gennaro S., Castillo-Toledo B., Di Benedetto M.D., Non-Linear Control of Electromagnetic Valves for Camless Engines. International Journal of Control, **80**, 11, 1796–1813, 2007.

[17]. M. Pettersson, L. Nielsen, "Gear shifting by engine control," Control Systems Technology, IEEE Transactions on, 8(3), 495-507, 2000.

[18]. Jonas Fredriksson, Bo Egardt, "Active engine control for gearshifting in automated manual transmissions, " International Journal of Vehicle Design, 32 (3-4), 216-230, 2003.

[19]. Rashad M., Tobias K., Gunther A., Ferit K., Modelling and Analysis of the Electro-Hydraulic and Driveline Control of a Dual Clutch Transmission. Proc. FISITA2010, Germany, 2010.

[20]. Merritt H., Hydraulic control systems. New York: Wiley, 1967.

[21]. Filicori F., Guarino Lo Bianco C., Tonielli A., "Modeling and control strategies for a variable reluctance direct-drive motor," IEEE Transactions on Industrial Electronics, 40(1), 105–115, 1993.

[22]. Goodson R., Leonard R., "A survey of modeling techniques for fluid line transients," ASME Journal of Basic Engineering, 94,474–482, 1972.

[23]. Lozano R., Brogliato B., Egeland O., Maschke B., Dissipative systems analysis and control. London: Springer, 2000.

[24]. Yang W., Tobler W. "Dissipative modal approximation of fluid transmission lines using linear friction model," ASME Journal of Dynamic Systems of Measurement and Control, 113, 152–162, 1991.